

Multiquark states at LHCb

Results and prospects

A. Augusto Alves Jr.

University of Cincinnati
aalvesju@cern.ch

Talk presented at

Dipartimento di Fisica dell'Università di Roma "La Sapienza", 30 November
2015



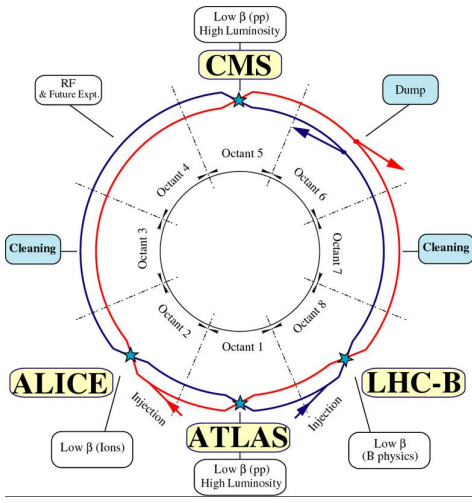
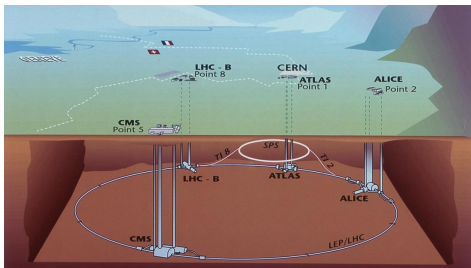
Outline

- ① The LHC accelerator and its detectors
- ② Exotic states
- ③ Results on $P(4380)^+_c$
- ④ Results on $Z(4430)^+$
- ⑤ $X(3872)$ quantum numbers and $\rho J/\psi$
- ⑥ Light meson spectroscopy
- ⑦ Conclusions

The LHC accelerator and its detectors

The LHC is designed to collide two high luminosity and high energy beams of protons or heavy ions.

- Two general purpose high luminosity experiments: CMS and ATLAS
- One low luminosity experiment, dedicated to flavour physics experiment: LHCb
- Heavy-ion experiment: ALICE



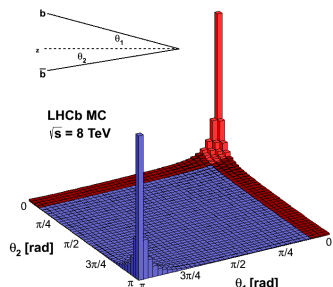
The LHC environment

During most of 2012 run, LHC collided protons at 8 TeV with an average instantaneous luminosity of $4 \times 10^{32} \text{ cm}^{-2} \text{s}^{-1}$ (LHCb) and 20 MHz of bunch crossing.

- Inelastic cross section $\sim 60 \text{ mb}$
- $\sigma(\text{pp} \rightarrow b\bar{b}X) = (284 \pm 20(\text{stat}) \pm 49(\text{syst})) \mu\text{b}$ [PLB 694, 209]
- $\Rightarrow \sim 10^6 B\bar{B}$ produced per second
- $\sigma(\text{pp} \rightarrow c\bar{c}X)$ is about 20 times higher. [Nucl.Phys. B871 (2013) 1-20]

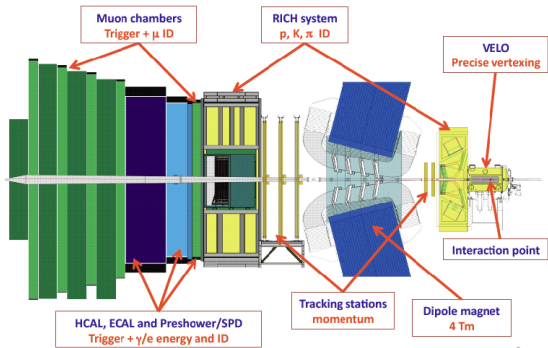
At the LHC energy, the $b\bar{b}$ pairs are produced preferentially at forward (backward) directions.

- 4π acceptance design is not optimal for flavour physics.
- Optimal solution is a forward detector: [LHCb](#)



The LHCb detector

LHCb experiment was designed to perform high precision flavour physics measurements at the LHC.



- **Good vertexing and tracking.** Precise primary and secondary vertex reconstruction. Excellent momentum, IP and proper time resolution.
- **Dataset.** $1 + 2 \text{ fb}^{-1}$ acquired in 2011 + 2012 runs

Quarkonia status

In QCD-motivated models, quarkonia states are basically described as $q\bar{q}$ pairs bound by a short-distance potential approximately Coulombic (single-gluon exchange) plus a linearly increasing confining potential at large separations.

- All charmonium states below the $D\bar{D}$ mass threshold have been observed.
- Charmonium states above the $D\bar{D}$ or $D\bar{D}^*$ mass threshold can decay into $D\bar{D}$ and $D\bar{D}^*$ final states.
- Many predicted states still not observed.
- Similar situation in the Beauty sector.

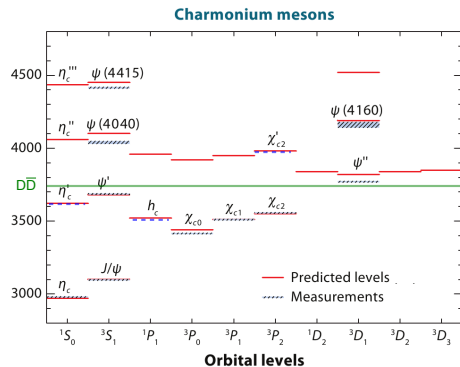


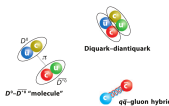
Figure from [Annu. Rev. Nucl. Part. Sci. 2008. 58:51–73]

XYZ states

Many new states have been observed at c-, b-factories and Tevatron

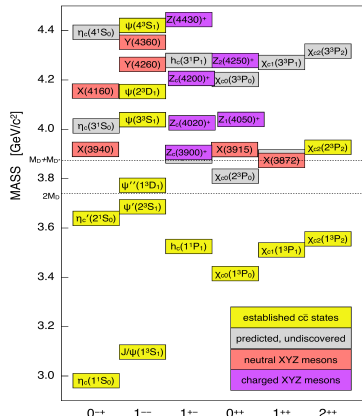
- Masses lying on the limits of the quarkonia spectrum
- Observed many different production mechanisms: ISR, e^+e^- , $\gamma\gamma$ and B decays.
- The measured masses do not correspond to the predicted values for conventional quarkonia.
- The properties do not fit very well to the quarkonia picture.

Many theoretical interpretations in discussion:



- conventional quarkonia;
- multiquark states;
- meson-molecules;
- hybrid mesons;
- threshold effects;

The table should be updated to include some new states: $P(4380)_c^+$, $P(4450)_c^+$...



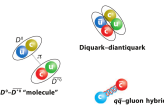
[PoS Bormio 050(2015) arXiv:1511.01589]

XYZ states

Many new states have been observed at Charm, B-factories and Tevatron

- Masses lying on the limits of the quarkonia spectrum
- Observed many different production mechanisms: ISR, e^+e^- , $\gamma\gamma$ and B decays.
- The measured masses do not correspond to the predicted values for conventional quarkonia.
- The properties do not fit very well to the quarkonia picture.

Many theoretical interpretations in discussion:



- conventional quarkonia;
- multiquark states;
- meson-molecules;
- hybrid mesons;
- threshold effects;

The table should be updated to include some new states: $P(4380)_c^+$, $P(4450)_c^+$...

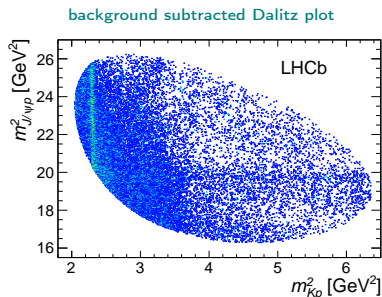
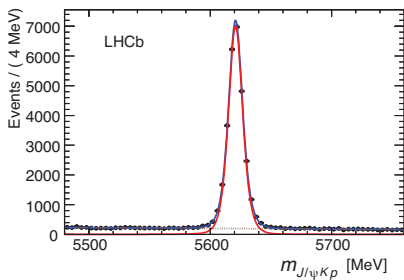
State	M (MeV)	Γ (MeV)	J^{PC}	Process (decay mode)
$X(3872)$	3871.68 ± 0.17	< 1.2	1^{++}	$B \rightarrow K + (J/\psi \pi^+ \pi^-)$ $p\bar{p} \rightarrow (J/\psi \pi^+ \pi^-) + \dots$ $B \rightarrow K + (J/\psi \pi^+ \pi^- \pi^0)$ $B \rightarrow K + (D^0 \bar{D}^0 \pi^0)$ $B \rightarrow K + (J/\psi \gamma)$ $B \rightarrow K + (\psi' \gamma)$ $pp \rightarrow (J/\psi \pi^+ \pi^-) + \dots$
$X(3915)$	3917.4 ± 2.7	28_{-9}^{+10}	0^{++}	$B \rightarrow K + (J/\psi \omega)$ $e^+ e^- \rightarrow e^+ e^- + (J/\psi \omega)$
$X(3940)$	3942_{-8}^{+9}	37_{-17}^{+27}	$0(?)^{-(?)^+}$	$e^+ e^- \rightarrow J/\psi + (D^* \bar{D})$ $e^+ e^- \rightarrow J/\psi + (\dots)$ $e^+ e^- \rightarrow \gamma + (D \bar{D})$ $e^+ e^- \rightarrow \gamma + (J/\psi \pi^+ \pi^-)$ $B \rightarrow K + (J/\psi \phi)$ $e^+ e^- \rightarrow J/\psi + (D^* \bar{D})$ $e^+ e^- \rightarrow \gamma + (J/\psi \pi^+ \pi^-)$ $e^+ e^- \rightarrow (J/\psi \pi^+ \pi^-)$ $e^+ e^- \rightarrow (J/\psi \pi^0 \pi^0)$
$Y(4360)$	4361 ± 13	74 ± 18	1^{--}	$e^+ e^- \rightarrow \gamma + (\psi' \pi^+ \pi^-)$
$X(4630)$	4634_{-11}^{+9}	92_{-32}^{+41}	1^{--}	$e^+ e^- \rightarrow \gamma (\Lambda_c^+ \bar{\Lambda}_c^-)$
$Y(4660)$	4664 ± 12	48 ± 15	1^{--}	$e^+ e^- \rightarrow \gamma + (\psi' \pi^+ \pi^-)$
$Z_c^+(3900)$	3890 ± 3	33 ± 10	1^{+-}	$Y(4260) \rightarrow \pi^+ + (J/\psi \pi^+)$ $Y(4260) \rightarrow \pi^- + (D \bar{D}^*)^+$
$Z_c^+(4020)$	4024 ± 2	10 ± 3	$1(?)^{+(?)^-}$	$Y(4260) \rightarrow \pi^- + (h_c \pi^+)$ $Y(4260) \rightarrow \pi^0 + (D^* \bar{D}^*)^+$
$Z_c^0(4020)$	4024 ± 4	10 ± 3	$1(?)^{+(?)^-}$	$Y(4260) \rightarrow \pi^0 + (h_c \pi^0)$
$Z_c^+(4050)$	4051_{-35}^{+24}	82_{-55}^{+51}	$?^{++}$	$B \rightarrow K + (\chi_c \pi^+)$
$Z_c^+(4200)$	4196_{-32}^{+35}	370_{-149}^{+99}	1^{+-}	$B \rightarrow K + (J/\psi \pi^+)$
$Z_c^+(4250)$	4248_{-6}^{+183}	177_{-72}^{+321}	$?^{++}$	$B \rightarrow K + (\chi_c \pi^+)$
$Z_c^+(4430)$	4477 ± 20	181 ± 31	1^{+-}	$B \rightarrow K + (\psi' \pi^+)$ $B \rightarrow K + (J/\psi \pi^+)$
$Y_b(10890)$	10888.4 ± 3.0	$30.7_{-7.7}^{+8.9}$	1^{--}	$e^+ e^- \rightarrow (\Upsilon(nS) \pi^+ \pi^-)$
$Z_b^+(10610)$	10607.2 ± 2.0	18.4 ± 2.4	1^{+-}	$\Upsilon(5S) \rightarrow \pi^- + (\Upsilon(1,2,3S) \pi^+)$ $\Upsilon(5S) \rightarrow \pi^- + (h_0(1,2P) \pi^+)$ $\Upsilon(5S) \rightarrow \pi^- + (B\bar{B}^*)^+$
$Z_b^0(10610)$	10609 ± 6		1^{+-}	$\Upsilon(5S) \rightarrow \pi^0 + (\Upsilon(1,2,3S) \pi^0)$
$Z_b^0(10650)$	10652.2 ± 1.5	11.5 ± 2.2	1^{+-}	$\Upsilon(5S) \rightarrow \pi^- + (\Upsilon(1,2,3S) \pi^-)$ $\Upsilon(5S) \rightarrow \pi^- + (h_0(1,2P) \pi^+)$ $\Upsilon(5S) \rightarrow \pi^- + (B^*\bar{B}^*)^+$

[PoS Bormio 050(2015) arXiv:1511.01589]

$$\Lambda_b^0 \rightarrow K^- \bar{p} J/\psi$$

Phys. Rev. Lett. 115 (2015) 072001

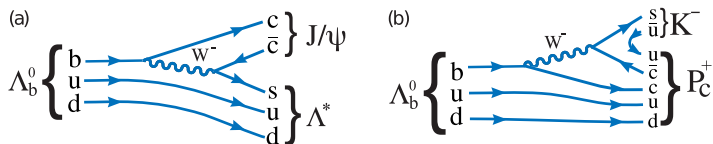
- Sample with $>26.000 \Lambda_b^0 \rightarrow K^- \bar{p} J/\psi$ signal candidates,
- Analysis: six-dimensional amplitude fit (invariant masses, helicity and decay planes angles).
- Background from sidebands. Estimated 5.4% of combinatorial background in the signal region.
- Six-dimensional efficiency calculated using complete simulation of the detector



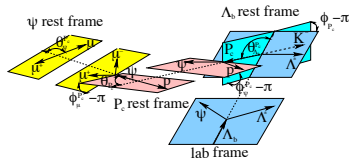
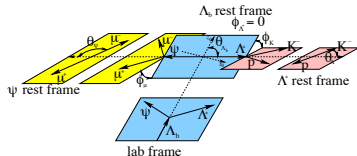
$$\Lambda_b^0 \rightarrow K^- p J/\psi$$

Some analysis details

- Two parametrizations: $\Lambda_b^0 \rightarrow K^-(P_c^+ \rightarrow p J/\psi)$ and $\Lambda_b^0 \rightarrow J/\psi(\Lambda^* \rightarrow p K^-)$, with $J/\psi \rightarrow \mu^+ \mu^-$



- Six-dimensional amplitude fit. Resonance invariant mass, three helicities angles, and two differences between decay planes.



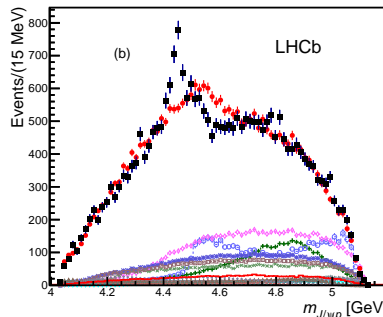
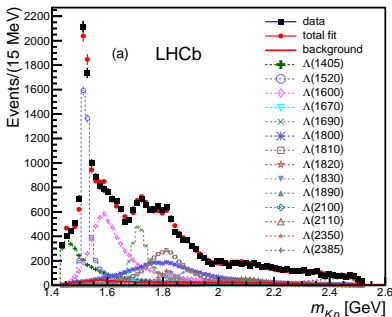
- Lorentz transformations relates the two helicity representantions.
 - Resonances described by Breit-Wigner.
 - Angular distribution calculated using helicity formalism.

$$\Lambda_b^0 \rightarrow K^- p J/\psi$$

Fit results without pentaquark states

- Fit including only Λ^* resonances, allowing all possible known states (Extended model)
 - The masses and widths of the Λ^* states are fixed to their PDG values
 - The m_{K_P} distribution is reasonably well fitted
 - The peaking structure in $m_{J/\psi P}$ is not described

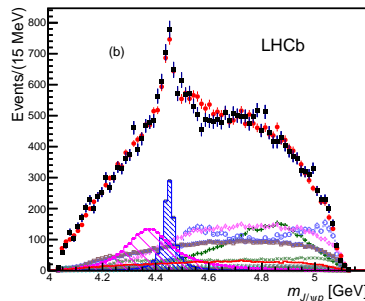
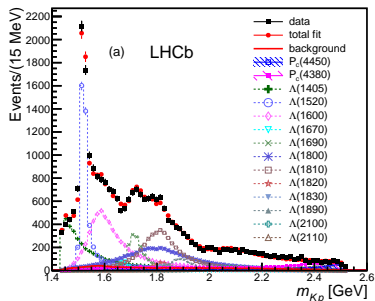
State	J^P	M_0 (MeV)	Γ_0 (MeV)	# Reduced	# Extended
$A(1405)$	$1/2^-$	$1405.1^{+1.3}_{-1.0}$	50.5 ± 2.0	3	4
$A(1520)$	$3/2^-$	1519.5 ± 1.0	15.6 ± 1.0	5	6
$A(1600)$	$1/2^+$	1600	150	3	4
$A(1670)$	$1/2^-$	1670	35	3	4
$A(1690)$	$3/2^-$	1690	60	5	6
$A(1800)$	$1/2^-$	1800	300	4	4
$A(1810)$	$1/2^+$	1810	150	3	4
$A(1820)$	$5/2^+$	1820	80	1	6
$A(1830)$	$5/2^-$	1830	95	1	6
$A(1890)$	$3/2^+$	1890	100	3	6
$A(2100)$	$7/2^-$	2100	200	1	6
$A(2110)$	$5/2^+$	2110	200	1	6
$A(2350)$	$9/2^+$	2350	150	0	6
$A(2585)$?	≈ 2585	200	0	6



$\Lambda_b^0 \rightarrow K^- p J/\psi$

Fit results with pentaquark states

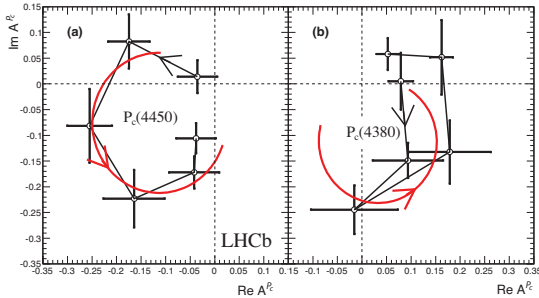
- Fit including just well motivated Λ^* resonances (Reduced model).
- Two P_c^+ states necessary to achieve acceptable fit quality.
- $P(4380)_c^+$ with $M = 4380 \pm 8 \pm 29 \text{ MeV}/c^2$ and $\Gamma = 205 \pm 18 \pm 86 \text{ MeV}/c^2$
 $J^P = 3/2^-$, fit fraction of $(8.4 \pm 0.7 \pm 4.2)\%$ and significance of 9σ
- $P(4450)_c^+$ with $M = 4449.8 \pm 1.7 \pm 2.5 \text{ MeV}/c^2$ and $\Gamma = 39 \pm 5 \pm 19 \text{ MeV}/c^2$
 $J^P = 5/2^+$, fit fraction $(4.1 \pm 0.5 \pm 1.1)\%$ and significance of 12σ
- The mass resolution is approximately $2.5 \text{ MeV}/c^2$ and combined significance 15σ
- Systematic uncertainties: see table in the backup slides.



$\Lambda_b^0 \rightarrow K^- p J/\psi$

Resonant character of the pentaquark state

- $P(4450)_c^+$ amplitude is now described by 6 independent complex numbers instead of a Breit-Wigner
- Six equidistant points in the range $\pm \Gamma_0 = 39 \text{ MeV}/c^2$ around $M_0 = 4449.8 \text{ MeV}/c^2$ (from the default fit)
- Observe a fast change of phase crossing maximum of magnitude. Expected behavior for a resonance.
- Same test on $P(4380)_c^+$ leads to inconclusive results

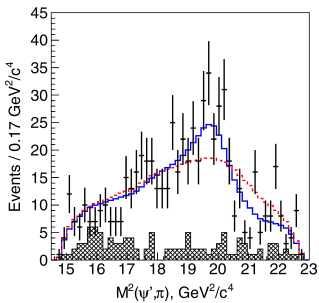


$Z(4430)^+$

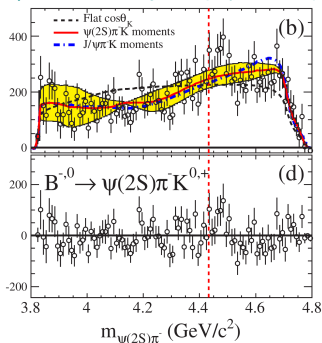
- Charged charmonium like state reported by Belle in $B^0 \rightarrow \psi(2S)K^+\pi^-$ decays [Phys.Rev.D88:074026]
- Searched and not confirmed or excluded by BaBar [Phys.Rev.D79:112001]
- Can not be explained as conventional meson.
- Minimum quark content: $c\bar{c}ud\bar{d}$
- No corresponding structure observed in $B^0 \rightarrow J/\psi K^+\pi^-$

$Z(4430)^+$ at Belle. K^{*0} and $K_2^*(1432)$ vetoed.

With $Z(4430)^+$ and No $Z(4430)^+$



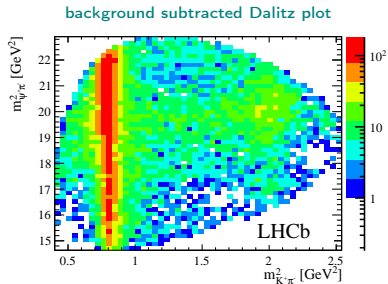
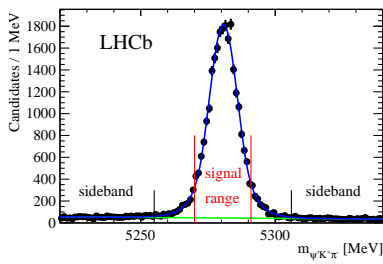
$Z(4430)^+$ at BaBar. Legendre polynomials approach.



Confirmation of $Z(4430)^+$ at LHCb

Phys.Rev.Lett.112, 222002 (2014)

- Sample with $>25.000 \ B^0 \rightarrow K^+\pi^-\psi(2S)$ signal candidates,
- Analysis performed using two different approaches:
 - Model dependent. Four-dimensional amplitude fit (invariant masses, helicity and decay planes angles).
 - Model independent. An analysis based on the Legendre polynomial moments extracted from the $K\pi$ system
- Background from sidebands. Estimated 4% of combinatorial background in the signal region.
- Four-dimensional efficiency calculated using complete simulation of the detector



$Z(4430)^+$

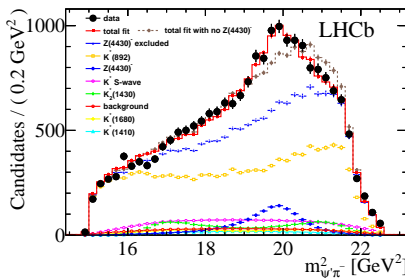
Amplitude fit

- Fitted parameters:

$$M_{Z(4430)^+} = 4475 \pm 7^{+15}_{-25} \text{ MeV}/c^2, \Gamma_{Z(4430)^+} = 172 \pm 13^{+37}_{-34} \text{ MeV}/c^2$$

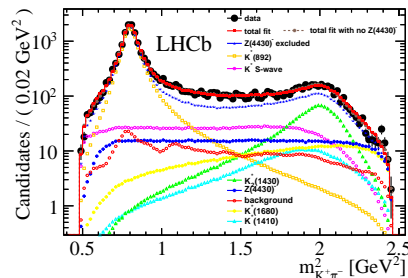
$$f_{Z(4430)^+} = (5.9 \pm 0.9^{+1.5}_{-3.3})\%$$

- Significance: $\Delta(-2\ln L) > 13.9\sigma$



A. A. Alves Jr

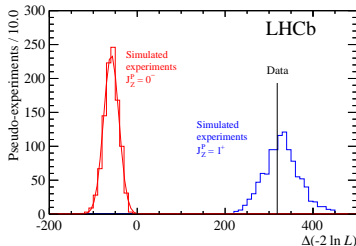
Multiquark states at LHCb



November 30, 2015

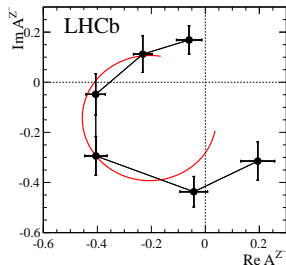
$Z(4430)^+$

Resonance character and spin determination



- $J^P = 1^+$ assignment favored.
- Other J^P assignments are ruled out with large significance: $> 9\sigma$

- $Z(4430)^+$ amplitude is described by 6 independent complex numbers instead of a Breit-Wigner
- Observe a fast change of phase crossing maximum of magnitude.
- Expected behaviour for a **resonance**.

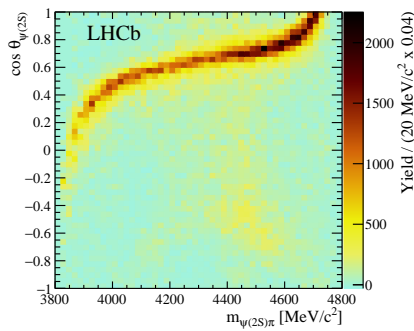
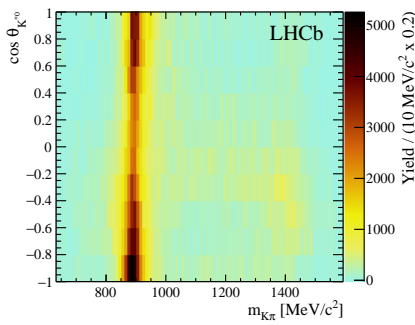


$Z(4430)^+$: model independent analysis

arXiv:1510.01951 (submitted to PRD)

The main goal is to check if the structures in the $m_{\psi(2S)\pi}$ spectrum can be explained as reflections of the resonance activity in the $K\pi$ system.

- No assumptions on the shape and coupling of the K^* resonances.
- Only its maximum J is restricted.

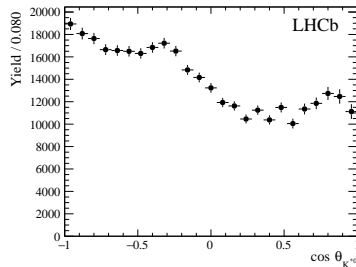
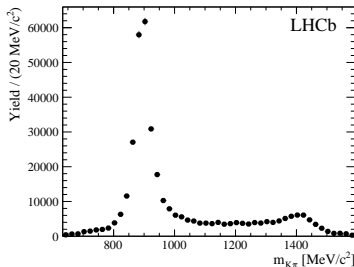


$Z(4430)^+$: model independent analysis

$K\pi$ system

- Very active $K\pi$ system.
- $m_{K\pi}$ taken directly from data, as it is.
- Angular structure of the $K\pi$ system acquired via Legendre polynomials.
- $\frac{dN}{d \cos \theta_{K^*0}} = \sum_{j=0}^{l_{\max}} \langle P_j^U \rangle P_j(\cos \theta_{K^*0})$
- $\langle P_j^U \rangle = \sum_{i=1}^{N_{\text{reco}}} \frac{W_i^{\text{signal}}}{e^i} P_j(\cos \theta_{K^*0}^i)$

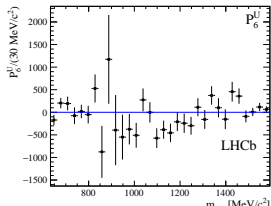
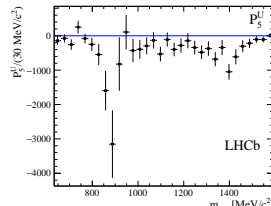
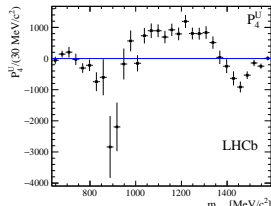
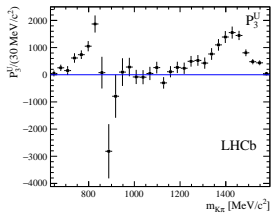
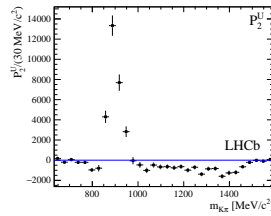
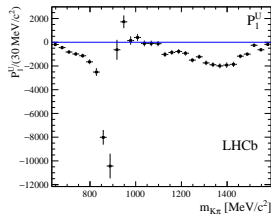
Resonance	Mass (MeV/c ²)	Γ (MeV/c ²)	J^P
$K^*(800)^0$	682±29	547±24	0^+
$K^*(892)^0$	895.81±0.19	47.4±0.6	1^-
$K^*(1410)^0$	1414±15	232±21	1^-
$K_0^*(1430)^0$	1425±50	270±80	0^+
$K_2^*(1430)^0$	1432.4±1.3	109±5	2^+
$K^*(1680)^0$	1717±27	322±110	1^-
$K_3^*(1780)^0$	1776±7	159±21	3^-



$Z(4430)^+$: model independent analysis

Legendre polynomial moments

The rich angular structure of the $K\pi$ system is shown by the very featured Legendre polynomial moments.

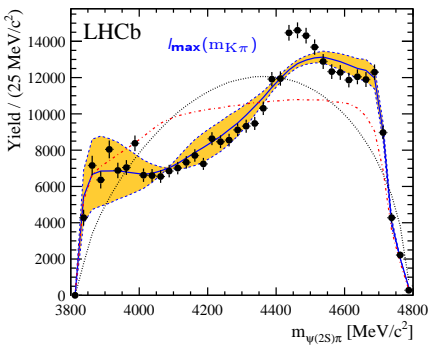


$Z(4430)^+$: model independent analysis

$m_{\psi(2S)\pi}$ spectrum

- The moments are normalized and used to predict, through a MC simulation, the expected $m_{\psi(2S)\pi}$ spectrum.
- The order of the Legendre polynomial expansion depends on the locally dominant $K\pi$ resonances

$$l_{\max}(m_{K\pi}) = \begin{cases} 2 & m_{K\pi} < 836 \text{ MeV}/c^2 \\ 3 & 836 \text{ MeV}/c^2 < m_{K\pi} < 1000 \text{ MeV}/c^2 \\ 4 & m_{K\pi} > 1000 \text{ MeV}/c^2. \end{cases}$$

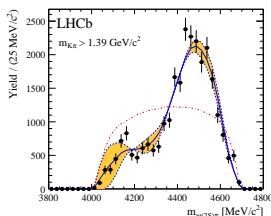
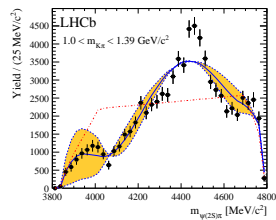
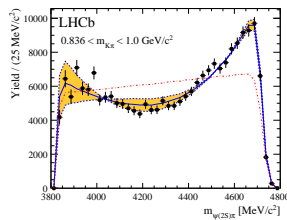
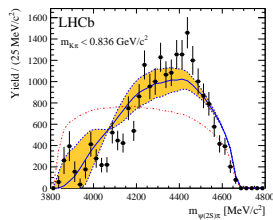


- Data points(black dots)
- MC prediction (blue solid line)
- Phase space MC (black dotted line)
- Phase space MC weighted to reproduce $m_{K\pi}$ (red line)

$Z(4430)^+$: model independent analysis

Slices of $m_{K\pi}$

Toy Monte Carlo prediction in slices of $m_{K\pi}$.

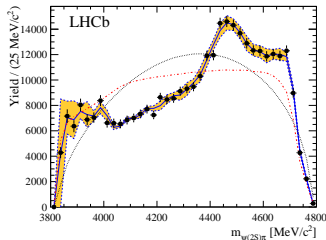


- Data points(black dots)
- MC prediction (blue solid line)
- Phase space MC weighted to reproduce $m_{K\pi}$ (red line)
- Clear disagreement between data and MC on the slice $1.0 < m_{K\pi} < 1.39 \text{ GeV}/c^2$

$Z(4430)^+$: model independent analysis

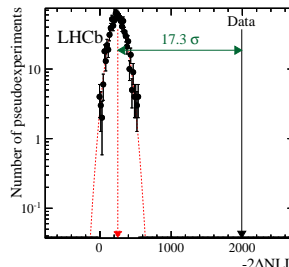
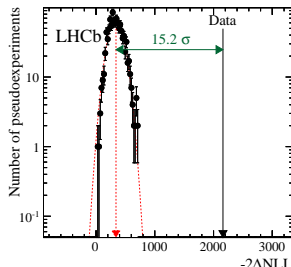
Hypothesis test

- Performed using a series of pseudo-experiments produced according with I_{\max} ($m_{K\pi}$).
- Hypothesis test based on likelihood ratio between I_{\max} ($m_{K\pi}$) and $I_{\max} = 30$.
- Efficiency effects and background subtraction taken into account in the pseudo-experiment generation.



full $m_{K\pi}$ spectrum

$1.0 < m_{K\pi} < 1.39 \text{ GeV}/c^2$

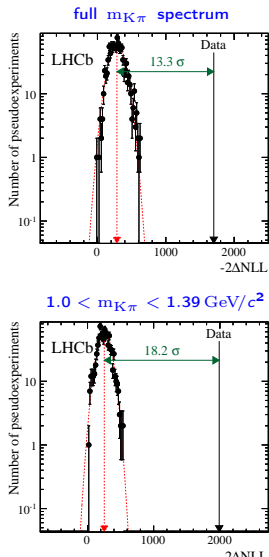
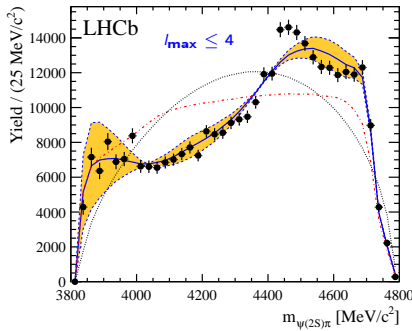


The hypothesis that the structure of the $m_{\psi(2S)\pi}$ spectrum can be described as a reflection of the activity of the resonances in the $K\pi$ system is ruled out with high significance.

$Z(4430)^+$: model independent analysis

Additional studies: $I_{\max} \leq 4$

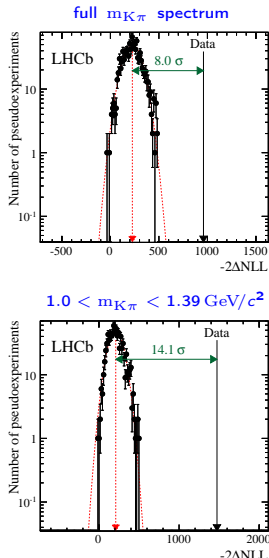
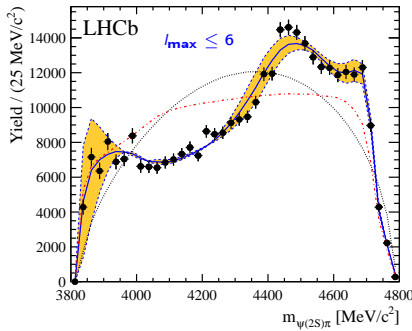
- Setting the maximum Legendre polynomial order to four, independent of $m_{K\pi}$
- This corresponds to suppose the $K\pi$ system has S,P and D waves contributing in all regions.
- Data can not be reproduced



$Z(4430)^+$: model independent analysis

Additional studies: $I_{\max} \leq 6$

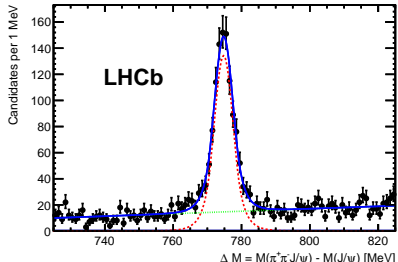
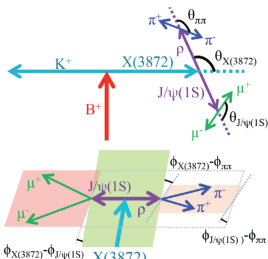
- Setting the maximum Legendre polynomial order to six, independent of $m_{K\pi}$
- This corresponds to suppose the $K\pi$ system has S, P, D and F waves contributing in all regions.
- Data still can not be reproduced



Quantum numbers of the X(3872) state and orbital angular momentum in its $\rho^0 J/\psi$ decays

Phys. Rev. D 92 (2015) 011102

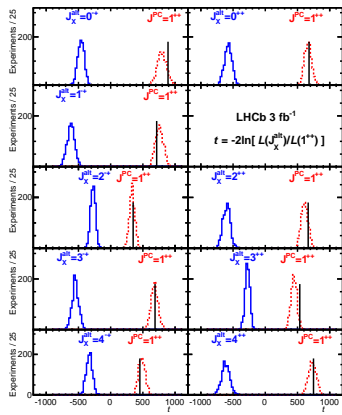
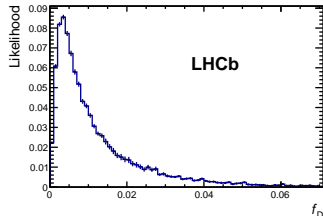
- Previous quantum number determinations assumed that the lowest orbital angular momentum between the X(3872) decay products dominated the matrix element.
- Significant contributions from higher orbital angular amplitudes could invalidate the 1^{++} assignment. **It is necessary to perform again the analysis allowing more general angular configurations.**
- Using the 3.0 fb^{-1} dataset recorded by LHCb in 2011 and 2012
- $1011 \pm 38 \text{ B}^+ \rightarrow K^+ X(3872)$ with $X(3872) \rightarrow J/\psi \pi^+ \pi^-$.
- 5D analysis: all angular correlations used to measure $X(3872) \ J^{PC}$



Quantum numbers of the X(3872) state and orbital angular momentum in its $\rho^0 J/\psi$ decays

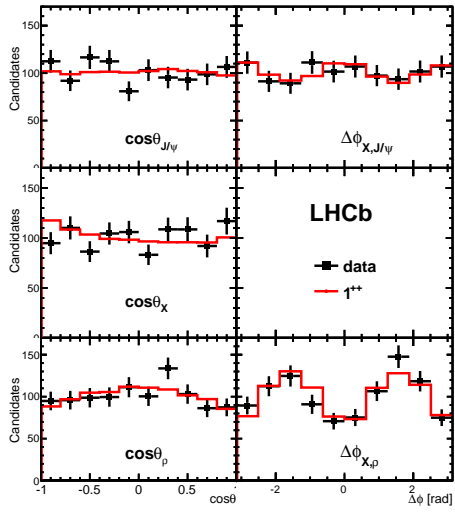
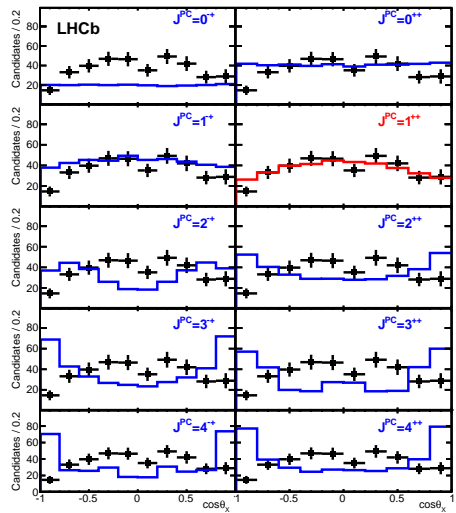
Hypothesis test

- A large set of X(3872) J^{PC} configurations is considered.
- Likelihood-ratio test to discriminate between the assignments against the 1^{++} ;
- Results on data compared to simulated experiments.
- Data favour the 1^{++} over the alternative hypothesis with $> 16.0\sigma$;
- No significant D-wave fraction is found, with an upper limit of 0.4% at 95% C.L.



Quantum numbers of the X(3872) state and orbital angular momentum in its $\rho^0 J/\psi$ decays

Angular distributions



$$B^0 \rightarrow J/\psi \pi^+ \pi^-$$

Phys. Rev. D 87, 052001

- The substructure of mesons belonging to the scalar nonet is controversial.
- Many possibilities: $q\bar{q}$, $q\bar{q}q\bar{q}$, mixtures etc.
- $q\bar{q}$ case:

$$|f_0(980)\rangle = \cos \varphi_m |s\bar{s}\rangle + \sin \varphi_m |n\bar{n}\rangle$$

$$|f_0(500)\rangle = -\sin \varphi_m |s\bar{s}\rangle + \cos \varphi_m |n\bar{n}\rangle,$$

$$\text{where } |n\bar{n}\rangle \equiv \frac{1}{\sqrt{2}} (|u\bar{u}\rangle + |d\bar{d}\rangle).$$

- $q\bar{q}q\bar{q}$ case:

$$|f_0(980)\rangle = \frac{1}{\sqrt{2}} (|[su][\bar{s}\bar{u}]\rangle + |[sd][\bar{s}\bar{d}]\rangle)$$

$$|f_0(500)\rangle = |[ud][\bar{u}\bar{d}]\rangle.$$

- Observable of interest for both cases:

$$\tan^2 \varphi_m \equiv r_\sigma^f = \frac{\mathcal{B}(\bar{B}^0 \rightarrow J/\psi f_0(980))}{\mathcal{B}(\bar{B}^0 \rightarrow J/\psi f_0(500))} \frac{\Phi(500)}{\Phi(980)}$$

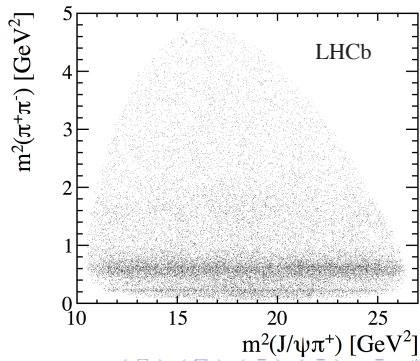
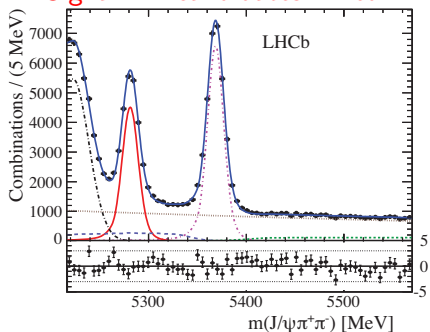
- Prediction for tetraquark states: $r_\sigma^f = 1/2$ [PRL 111, 062001 (2013)]

$B^0 \rightarrow J/\psi \pi^+ \pi^-$

Amplitude analysis

- Approach similar to the $Z(4430)^+$ analysis: 4D matrix element describing $\pi^+ \pi^-$ resonances;
- No evidence of $J/\psi \pi^+$ resonances
- 19,000 B^0 signal candidates
- Background modelled from sidebands

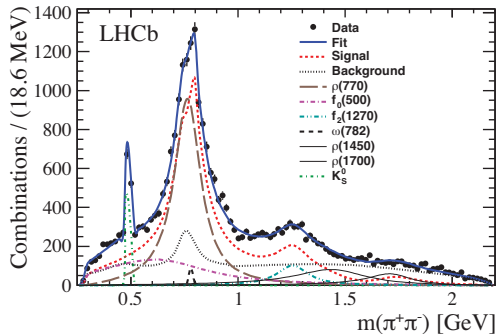
Signal B^0 candidates in red.



$B^0 \rightarrow J/\psi \pi^+ \pi^-$

Results

R	$\mathcal{B}(\bar{B}^0 \rightarrow J/\psi R, R \rightarrow \pi^+ \pi^-)$
$\rho(770)$	$(2.50 \pm 0.10^{+0.18}_{-0.15}) \times 10^{-5}$
$f_0(500)$	$(8.8 \pm 0.5^{+1.1}_{-1.5}) \times 10^{-6}$
$f_2(1270)$	$(3.0 \pm 0.3^{+0.2}_{-0.3}) \times 10^{-6}$
$\omega(782)$	$(2.7^{+0.8+0.7}_{-0.6-0.5}) \times 10^{-7}$
$\rho(1450)$	$(4.6 \pm 1.1 \pm 1.9) \times 10^{-6}$
$\rho(1700)$	$(2.0 \pm 0.5 \pm 1.2) \times 10^{-6}$



- Best fit model shows does not require $f_0(980)$ component.
- Upper limit on the $f_0(500) - f_0(980)$ mixing angle.
- Different from tetraquark prediction (1/2) by 8σ

$$\tan^2 \varphi_m \equiv r_\sigma^f = (1.1^{+1.2+6.0}_{-0.7-0.7}) \times 10^{-2} < 0.098 \text{ at 90\% C.L.}$$

Multiquark states spectroscopy at LHCb

Previous results and prospects

Previous results:

- X(3872) mass and production cross-section measurements [Eur. Phys. J. C 72 (2012) 1972]. There is work in progress to update the mass measurement using the full dataset.
- X(3872) quantum numbers determination [Phys. Rev. Lett. 110, 222001 (2013)]. In this analysis the decay of X(3872) was supposed to proceed only via $\rho J/\psi$ S wave. Updated result discussed in the previous slides.
- Search for X(3872) and X(3915) in $B^+ \rightarrow K^+ p\bar{p}$ [Eur.Phys.J. C73 (2013) 2462].
- Evidence of $X(3872) \rightarrow \psi(2S)\gamma$ [Nuclear Physics B 886 (2014) 665-680]. Update with 2016 statistics.
- Results on X(4140) and X(4274) at LHCb [Phys. Rev. D 85,091103(R)(2012)]. Full amplitude analysis in progress using the full dataset.

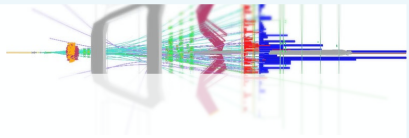
There is intensive activity inside the LHCb searching for new multiquark candidates.

Many other results in b and c spectroscopy

Access: http://lhcbproject.web.cern.ch/lhcbproject/Publications/LHCbProjectPublic/Summary_all.html



The LHCb Public results



LHCb publications

[to restricted-access page]

PUBLICATIONS PER WORKING GROUP

FLAVOUR TAGGING

b-HADRONS AND QUARKONIA

B DECAYS TO CHARMONIUM

DETECTOR PERFORMANCE

CHARMLESS b-HADRON DECAYS

QCD, ELECTROWEAK AND EXOTICA

RARE DECAYS

CHARM PHYSICS

SEMILEPTONIC B DECAYS

LUMINOSITY

B DECAYS TO OPEN CHARM

List of papers (Total of 284 papers)

TITLE	DOCUMENT NUMBER	JOURNAL	SUBMITTED ON
Search for the rare decays $B^0 \rightarrow J/\psi \gamma$ and $B_s^0 \rightarrow J/\psi \gamma$	PAPER-2015-044	PRD	16 Oct 2015
Evidence for the strangeness-changing weak decay $\Xi_b^- \rightarrow \Lambda_b^0 \pi^-$	PAPER-2015-047	PRL	13 Oct 2015
A model-independent confirmation of the $Z(4430)^+$ state	PAPER-2015-038	PRD	07 Oct 2015
Measurements of prompt charm production cross-sections in $p\bar{p}$ collisions at $\sqrt{s} = 13\text{ TeV}$	PAPER-2015-041	JHEP	06 Oct 2015
Model-independent measurement of mixing parameters in $D^0 \rightarrow K_S \pi^+ \pi^-$ decays	PAPER-2015-042	JHEP	06 Oct 2015
Measurement of the forward-backward asymmetry in $Z/\gamma^* \rightarrow \mu^+ \mu^-$ decays and determination of the effective weak mixing angle	PAPER-2015-039	JHEP	25 Sep 2015
Studies of the resonance structure in $D^0 \rightarrow K_S^0 K^+ \pi^-$ decays	PAPER-2015-026	PRD	22 Sep 2015
Forward production of T meson in $p\bar{p}$ collisions at $\sqrt{s} = 7$ and 8 TeV	PAPER-2015-045	JHEP	08 Sep 2015
Measurement of forward J/ψ production cross-sections in $p\bar{p}$ collisions at $\sqrt{s} = 13\text{ TeV}$	PAPER-2015-037	JHEP	02 Sep 2015
First measurement of the differential branching fraction and CP asymmetry of the $B^+ \rightarrow \pi^+ \mu^+ \mu^-$ decay	PAPER-2015-035	JHEP	01 Sep 2015
Measurement of CP violation parameters and polarisation fractions in $B_s^0 \rightarrow J/\psi \bar{K}^{*-0}$ decays	PAPER-2015-034	JHEP	01 Sep 2015
Study of the production of Λ_b^0 and $\bar{\Lambda}_b^0$ hadrons in $p\bar{p}$ collisions and first measurement of the $\Lambda_b^0 \rightarrow J/\psi \bar{K}^-$ branching fraction	PAPER-2015-032	Chin Phys C	01 Sep 2015
Measurement of the time-integrated CP asymmetry in $D^0 \rightarrow K_S^0 K_S^0$ decays	PAPER-2015-030	JHEP	25 Aug 2015
Search for hidden-sector bosons in $B^0 \rightarrow K^{*0} \mu^+ \mu^-$ decays	PAPER-2015-036	PRL	17 Aug 2015
Measurement of the $B_s^0 \rightarrow \phi \phi$ branching fraction and search for the decay $B^0 \rightarrow \phi \phi$	PAPER-2015-028	JHEP	04 Aug 2015
B flavour tagging using charm decays at the LHCb experiment	PAPER-2015-027	JINST	28 Jul 2015
Measurement of the branching fraction ratio $B(B_s^+ \rightarrow \psi(2S)\pi^+)/B(B_s^+ \rightarrow J/\psi\pi^+)$	PAPER-2015-024	PRD	13 Jul 2015
Observation of $J/\psi p$ resonances consistent with pentaquark states in $\Lambda_b^0 \rightarrow J/\psi \bar{K}^- p$ decays	PAPER-2015-029	Phys. Rev. Lett. 115 (2015) 072001	13 Jul 2015
Search for long-lived heavy charged particles using a ring imaging Cherenkov technique at LHCb	PAPER-2015-002	JHEP	30 Jun 2015
Angular analysis and differential branching fraction of the decay $B_s^0 \rightarrow \phi \mu^+ \mu^-$	PAPER-2015-023	JHEP	29 Jun 2015

Summary

$P(4380)_c^+$ and $P(4450)_c^+$

- $P(4380)_c^+$ observed with 9.0σ in multidimensional amplitude fit. Quantum numbers $J^P = 3/2^-$
- $P(4450)_c^+$ observed with 12.0σ in multidimensional amplitude fit. Quantum numbers $J^P = 5/2^+$
- Resonance behavior observed for $P(4450)_c^+$. $P(4380)_c^+$ needs further studies.

$Z(4430)^+$

- Existence confirmed with $> 13.0\sigma$ in multidimensional amplitude fit.
- Existence confirmed with $> 8.0\sigma$ in model independent analysis.
- Quantum numbers determination $J^P = 1^+$
- Resonant behavior observed.

Summary

X(3872) quantum numbers

- Analysis of the X(3872) quantum numbers using full LHCb dataset
- Determination of the $\rho J/\psi$ D wave fraction.

Light quark spectroscopy using $B^0 \rightarrow J/\psi \pi^+ \pi^-$

- No evidence for $f_0(980)$ resonance production
- $f_0(980)$ as a tetraquark state ruled out at 8σ

Thanks!

Backup

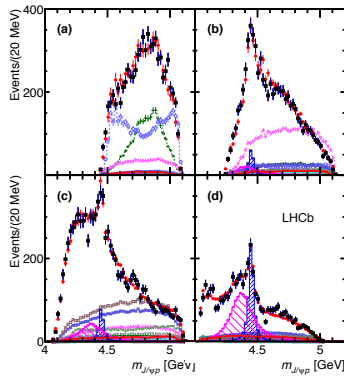
$\Lambda_b^0 \rightarrow K^- p J/\psi$: Systematic uncertainties

Table 2: Summary of systematic uncertainties on P_c^+ masses, widths and fit fractions, and Λ^* fit fractions. A fit fraction is the ratio of the phase space integrals of the matrix element squared for a single resonance and for the total amplitude. The terms “low” and “high” correspond to the lower and higher mass P_c^+ states. The sFit/cFit difference is listed as a cross-check and not included as an uncertainty.

Source	M_0 (MeV)		Γ_0 (MeV)		Fit fractions (%)			
	low	high	low	high	low	high	$\Lambda(1405)$	$\Lambda(1520)$
Extended vs. reduced	21	0.2	54	10	3.14	0.32	1.37	0.15
Λ^* masses & widths	7	0.7	20	4	0.58	0.37	2.49	2.45
Proton ID	2	0.3	1	2	0.27	0.14	0.20	0.05
$10 < p_p < 100$ GeV	0	1.2	1	1	0.09	0.03	0.31	0.01
Nonresonant	3	0.3	34	2	2.35	0.13	3.28	0.39
Separate sidebands	0	0	5	0	0.24	0.14	0.02	0.03
J^P ($3/2^+, 5/2^-$) or ($5/2^+, 3/2^-$)	10	1.2	34	10	0.76	0.44		
$d = 1.5 - 4.5$ GeV $^{-1}$	9	0.6	19	3	0.29	0.42	0.36	1.91
$L_{\Lambda_b^0}^{P_c} \Lambda_b^0 \rightarrow P_c^+ (\text{low/high}) K^-$	6	0.7	4	8	0.37	0.16		
$L_{P_c}^{P_c^+} (\text{low/high}) \rightarrow J/\psi p$	4	0.4	31	7	0.63	0.37		
$L_{\Lambda_b^0}^{A_n^*} \Lambda_b^0 \rightarrow J/\psi \Lambda^*$	11	0.3	20	2	0.81	0.53	3.34	2.31
Efficiencies	1	0.4	4	0	0.13	0.02	0.26	0.23
Change $\Lambda(1405)$ coupling	0	0	0	0	0	0	1.90	0
Overall	29	2.5	86	19	4.21	1.05	5.82	3.89
sFit/cFit cross check	5	1.0	11	3	0.46	0.01	0.45	0.13

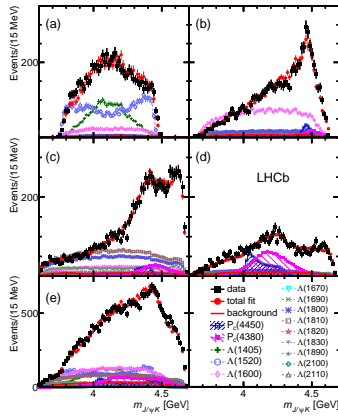
$\Lambda_b^0 \rightarrow K^- p J/\psi$: Slices $m_{pJ/\psi}$

Figure 8: $m_{J/\psi p}$ in various intervals of m_{Kp} for the fit with two P_c^+ states: (a) $m_{Kp} < 1.55$ GeV, (b) $1.55 < m_{Kp} < 1.70$ GeV, (c) $1.70 < m_{Kp} < 2.00$ GeV, and (d) $m_{Kp} > 2.00$ GeV. The data are shown as (black) squares with error bars, while the (red) circles show the results of the fit. The blue and purple histograms show the two P_c^+ states. See Fig. 7 for the legend.



$\Lambda_b^0 \rightarrow K^- p J/\psi$: Slices $m_{KJ/\psi}$

Figure 11: Projections onto $m_{J/\psi K}$ in various intervals of m_{Kp} for the reduced model fit (cFit) with two P_c^+ states of J^P equal to $3/2^-$ and $5/2^+$: (a) $m_{Kp} < 1.55$ GeV, (b) $1.55 < m_{Kp} < 1.70$ GeV, (c) $1.70 < m_{Kp} < 2.00$ GeV, (d) $m_{Kp} > 2.00$ GeV, and (e) all m_{Kp} . The data are shown as (black) squares with error bars, while the (red) circles show the results of the fit. The individual resonances are given in the legend.



Backup: Older results

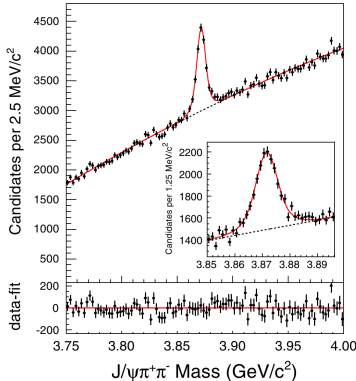
X(3872)

The X(3872) exotic-meson was discovered in 2003 by the Belle collaboration in $B \rightarrow K X(3872)$ with $X(3872) \rightarrow J/\psi \pi^+ \pi^-$.

- Its existence was immediately confirmed by BaBar, CDF, DØ collaborations.
- Quantum numbers previously constrained to 1^{++} or 2^{-+} . It were just measured by LHCb as 1^{++} .
- Clear signature on the $X(3872) \rightarrow J/\psi \pi^+ \pi^-$ mode. $\pi^+ \pi^-$ mass spectrum well studied.
- Mass known to $0.2 \text{ MeV}/c^2$ and width $< 1.2 \text{ MeV}/c^2$.

X(3872) signal at CDF

PRL 103,152001 (2009)



The nature of the X(3872) remains uncertain:

- Conventional charmonium $\chi_{c1}(2^3P_1)$. (very unlikely)
- Mesonic molecular state: $D^{*0} \bar{D}^0$ bound state.
- Tetraquark (diquark-anti-diquark).

X(3872) production studies at LHCb

At LHCb, the X(3872) can be studied using:

- Prompt candidates: higher statistics but large combinatorial background.
- Candidates from B decays: lower statistics but more clear samples
- Both kinds of candidates (inclusive selection)

X(3872) production studies at LHCb:

- Measure $\sigma(pp \rightarrow X(3872) + \dots) \times \mathcal{B}(X(3872) \rightarrow J/\psi \pi^+ \pi^-)$
- X(3872) taken as a 1^{++} state
- Inclusive selection of $X(3872) \rightarrow J/\psi \pi^+ \pi^-$
- Fiducial range: $5 < p_T < 20$ GeV and $2.5 < y < 4.5$
- Efficiency estimated from Monte Carlo

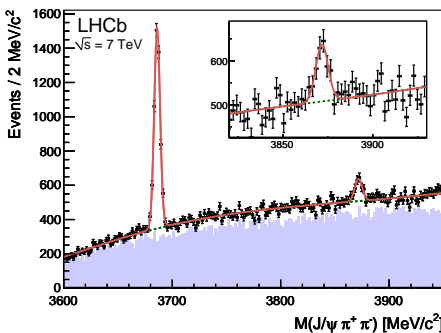
X(3872) production studies at LHCb

[Eur. Phys. J. C. 72 (2012) 1972]

Analysis performed on data sample with integrated luminosity of 34.7 pb^{-1} collected by the LHCb experiment in pp collisions at $\sqrt{s} = 7 \text{ TeV}$ in 2010.

$$\sigma(\text{pp} \rightarrow \text{X}(3872) + \dots) \times \mathcal{B}(\text{X}(3872) \rightarrow \text{J}/\psi \pi^+ \pi^-) = 5.4 \pm 1.3(\text{stat}) \pm 0.8(\text{syst}) \text{ nb}$$

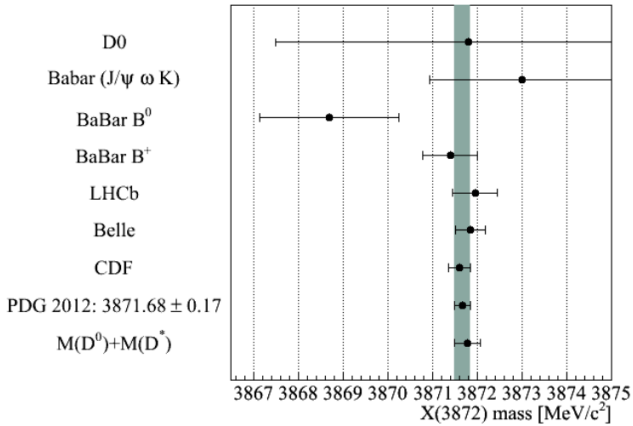
$$M(\text{X}(3872)) = 3871.95 \pm 0.48(\text{stat}) \pm 0.12(\text{syst}) \text{ MeV}/c^2$$



- 585 ± 74 X(3872) signal candidates
- Momentum scale calibration using $\text{J}/\psi \rightarrow \mu^+ \mu^-$.
- X(3872) peak fitted with fixed width.
- Background studied from wrong-sign pions combinations and modeled by exponential function.
- Uncertainty dominated by statistics. It will improve with 2011 dataset

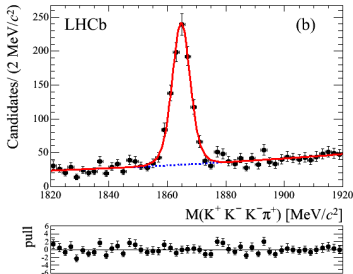
Status of X(3872) mass

- World average and $D^0\bar{D}^0$ -threshold are indistinguishable.
- Mass is a critical parameter for the $D^0\bar{D}^0$ -bound state hypothesis.
- Very low binding energy: $E_{bind} = 0.16 \pm 0.26 \text{ MeV}/c^2$



Precision D^0 mass measurement at LHCb

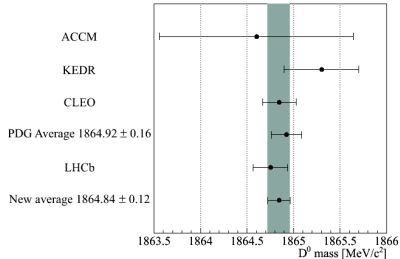
JHEP 1306 (2013) 065



- D^0 mass measurement using D produced in semileptonic B decays
- Using $D^0 \rightarrow K^+ K^- K^+ \pi^-$
- 846 ± 36 events, low Q , low systematics

$$M(D^0) = 1864.75 \pm 0.15(\text{stat}) \pm 0.11(\text{syst}) \text{ MeV}/c^2$$

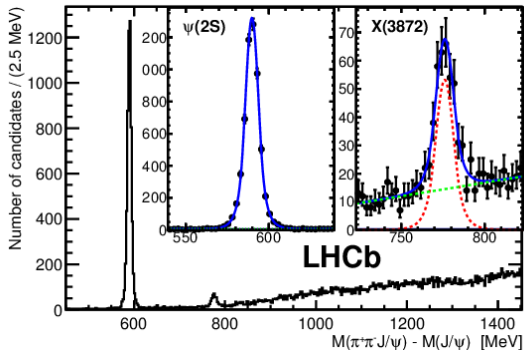
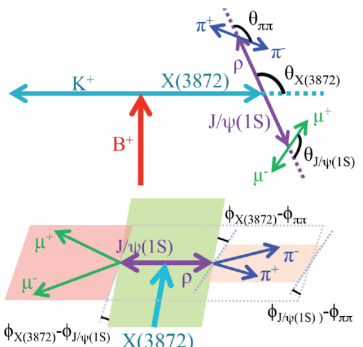
- This result reinforces that if $X(3872)$ is a $D^0 \bar{D}^{0*}$ bound-state, it is loosely bound.
- Consistent with arxiv:1212.4191:
 $M(D^0) = 1864.851 \pm 0.020(\text{stat})$



X(3872) quantum numbers determination

Phys. Rev. Lett. 110, 222001 (2013)

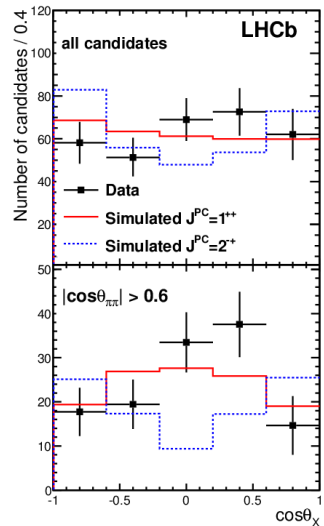
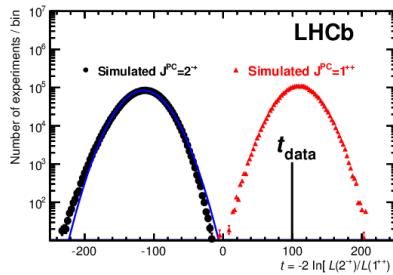
- Using the 1.0 fb^{-1} dataset recorded by LHCb in 2011
- $313 \pm 26 \text{ B}^+ \rightarrow K^+ X(3872)$ with $X(3872) \rightarrow J/\psi \pi^+ \pi^-$.
- $5642 \pm 76 \text{ B}^+ \rightarrow K^+ \psi(2S)$ with $\psi(2S) \rightarrow J/\psi \pi^+ \pi^-$.
- 5D analysis: all angular correlations used to measure $X(3872) \ J^{PC}$



X(3872) quantum numbers determination

Phys. Rev. Lett. 110, 222001 (2013)

- Two X(3872) J^{PC} configurations are considered: 1^{++} and 2^{-+} ;
- Likelihood-ratio test, to discriminate between the assignments;
- Compare the results to simulated experiments;
- Data favour the 1^{++} over the 2^{-+} hypothesis at 8.4σ ;

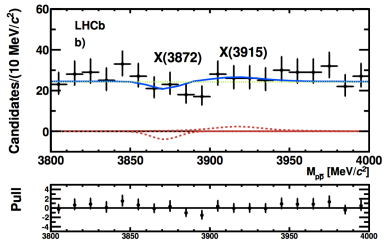
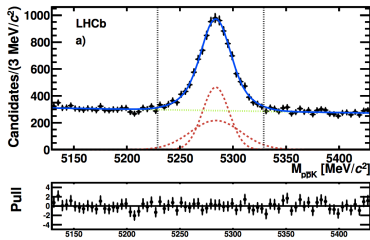


This result favours the interpretations of X(3872) as an exotic state.

Search for X(3872) and X(3915) in $B^+ \rightarrow K^+ p\bar{p}$

Eur.Phys.J. C73 (2013) 2462

- Search for $B \rightarrow KX(3872)$ with $X(3872) \rightarrow p\bar{p}$;
- 6951 ± 176 candidates of $B^+ \rightarrow K^+ p\bar{p}$
- $-9 \pm 8(\text{stat}) \pm 2(\text{syst})$ candidates of $X(3872) \rightarrow p\bar{p}$
- $13 \pm 17(\text{stat}) \pm 5(\text{syst})$ candidates of $X(3915) \rightarrow p\bar{p}$
- $\frac{\mathcal{B}(B^+ \rightarrow K^+ X(3872)) \times \mathcal{B}(X(3872) \rightarrow p\bar{p})}{\mathcal{B}(B^+ \rightarrow K^+ J/\psi) \times \mathcal{B}(J/\psi \rightarrow p\bar{p})} < 0.008 @ 95\% CL$
- $\frac{\mathcal{B}(B^+ \rightarrow K^+ X(3872)) \times \mathcal{B}(X(3915) \rightarrow p\bar{p})}{\mathcal{B}(B^+ \rightarrow K^+ J/\psi) \times \mathcal{B}(J/\psi \rightarrow p\bar{p})} < 0.032 @ 95\% CL$



Evidence of $X(3872) \rightarrow \psi(2S)\gamma$

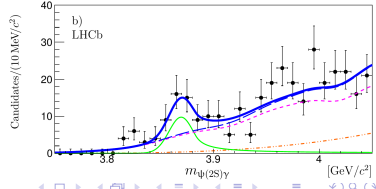
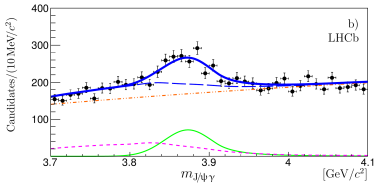
Nuclear Physics B 886 (2014) 665-680

Radiative decays of the $X(3872)$ provide a valuable opportunity to understand its nature.

- The $X(3872)$ C-parity has been determined studying the $X(3872) \rightarrow \gamma J/\psi$ decay.
- $R_{\psi\gamma} = \frac{\mathcal{B}(X(3872) \rightarrow \psi(2S)\gamma)}{\mathcal{B}(X(3872) \rightarrow J/\psi\gamma)}$ can give information about the internal structure of $X(3872)$.

- Analysis performed using 3 fb^{-1} collected in 2011 and 2012.
- Observed 4.4σ evidence of $X(3872) \rightarrow \psi(2S)\gamma$ in $B^+ \rightarrow K^+ X(3872)$ decays.

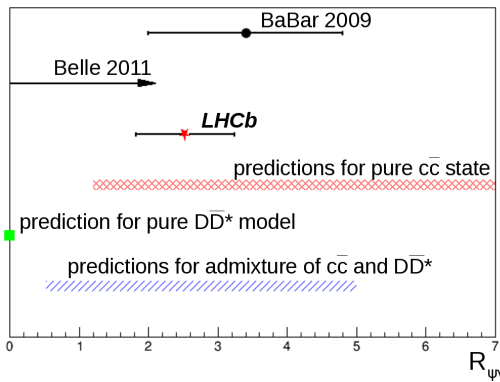
Parameter	Decay mode	
	$X(3872) \rightarrow J/\psi\gamma$	$X(3872) \rightarrow \psi(2S)\gamma$
m_{B^+} [MeV/ c^2]	5277.7 ± 0.8	5281.9 ± 2.4
$m_{X(3872)}$ [MeV/ c^2]	3873.4 ± 3.4	3869.5 ± 3.4
N_ψ	591 ± 48	36.4 ± 9.0



Evidence of $X(3872) \rightarrow \psi(2S)\gamma$

Nuclear Physics B 886 (2014) 665-680

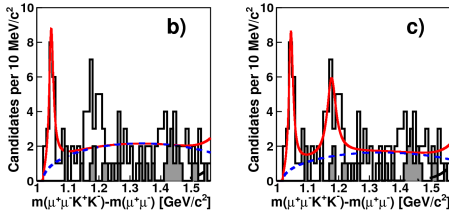
- $R_{\psi(2S)\gamma} = \frac{\mathcal{B}(X(3872) \rightarrow \psi(2S)\gamma)}{\mathcal{B}(X(3872) \rightarrow J/\psi\gamma)} = 2.46 \pm 0.64 \pm 0.29$
- These results disfavours $D^{*0}\bar{D}^0$ molecule hypothesis



The X(4140) and X(4274) candidates

Two exotic resonance candidates observed by CDF in $B^\pm \rightarrow J/\psi \phi K^\pm$ decays and decaying into $J/\psi \phi$.

[Ref. Phys.Rev.Lett. 102.242002, arXiv:1101.6058].



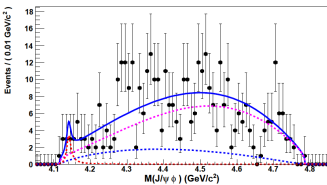
- 115 ± 12 candidates of $B^\pm \rightarrow J/\psi \phi K^\pm$
- X(4140) candidate with $M_{X(4140)} = 4143.4^{+2.9}_{-3.0} \pm 0.6 \text{ MeV}/c^2$,
 $\Gamma_{X(4140)} = 15.3^{+10.4}_{-6.1} \pm 2.5 \text{ MeV}/c^2$, with yield of 19 ± 6 and statistical significance of 5.0σ .
- Maybe a second state: $M_{X(4274)} = 4274.4^{+8.4}_{-6.4} \pm 1.9 \text{ MeV}/c^2$,
 $\Gamma_{X(4274)} = 32.3^{+21.9}_{-15.3} \pm 7.6 \text{ MeV}/c^2$, with yield of 22 ± 8 and statistical significance of 3.1σ .
- CDF results imply:

$$\mathcal{B}(B^+ \rightarrow X(4140)K^+) \times \mathcal{B}(X(4140) \rightarrow J/\psi \phi) = (5.2 \pm 1.7) \times 10^{-5}$$

The X(4140) and X(4274) candidates

Belle experiment also have searched for X(4140) and X(4274)

[see J. Brodzicka, Heavy flavour spectroscopy (LP09)]



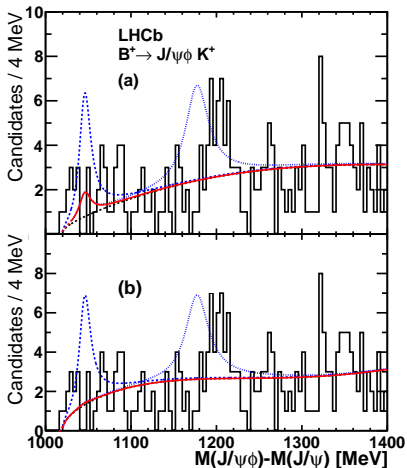
- Belle accumulated more events on $B^+ \rightarrow J/\psi \phi K^+$ than CDF but could not confirm or exclude the X(4140).
- Loss of efficiency near the threshold resulted in a lower sensitivity to X(4140) at Belle.
- $\mathcal{B}(B^+ \rightarrow X(4140)K^+) \times \mathcal{B}(X(4140) \rightarrow J/\psi \phi) < 6 \times 10^{-6}$

In summary:

- Charmonium states at this mass are expected to have much larger widths because of open flavour decay channels.
- Their decay rate into the $J/\psi \phi$ mode (so near the kinematic threshold) should be small and unobservable.
- Then, the observation by CDF has triggered much theoretical interest about the nature of this candidates.
- The existence of X(4140) and X(4274) candidates remains unconfirmed.

Search for X(4140) and X(4274)

- The LHCb sensitivity to X(4140) signal is a factor two better than in CDF.
- According the CDF results, we should observe 35 ± 11 X(4140) signal candidates and 53 ± 19 X(4274) signal candidates.
- No narrow structure is observed near the threshold.
- The fit shown in (a) gives a X(4140) yield of 6.9 ± 4.9 events and a X(4274) yield of $3.4^{+6.5}_{-3.4}$ events.
- The fit shown in (b) gives a X(4140) yield of 0.6 events with a positive error of 7.1 events and zero signal X(4274) events with a positive error of 10.



- The solid red line represents the result of the fit to our data.
- The dashed blue line represents the the expected signal amplitude from the CDF results.
- The top and bottom plots background functions are:
 - a) efficiency-corrected three-body phase-space;
 - b) quadratic polynomial.

Results on X(4140) and X(4274) at LHCb

Phys. Rev. D 85,091103(R)(2012)

The results of the search for X(4140) and X(4274) at LHCb are the two following limits calculated at 90%CL:

$\frac{\mathcal{B}(B^+ \rightarrow X(4140)K^+) \times \mathcal{B}(X(4140) \rightarrow J/\psi\phi)}{\mathcal{B}(B^+ \rightarrow J/\psi\phi K^+)}$		
LHCb(a)	LHCb(b)	CDF
< 0.07	< 0.04	$0.149 \pm 0.039 \pm 0.024$

$\frac{\mathcal{B}(B^+ \rightarrow X(4274)K^+) \times \mathcal{B}(X(4274) \rightarrow J/\psi\phi)}{\mathcal{B}(B^+ \rightarrow J/\psi\phi K^+)}$	
LHCb	CDF (our estimate)
< 0.08	0.17 ± 0.06

In conclusion, LHCb performed the most sensitive search for the narrow X(4140) and X(4274) structures and:

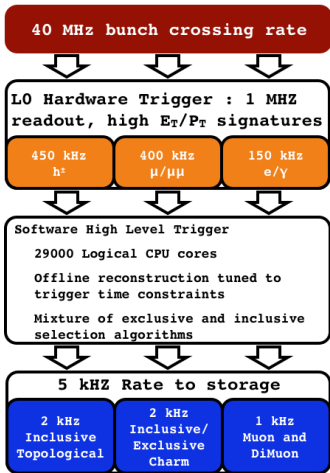
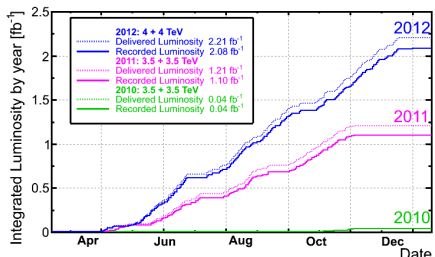
- Does not confirm the X(4140) state previously reported by the CDF
- Does not observe any evidence of the X(4274)
- The LHCb results disagree at the 2.4σ level with the CDF measurement.

Backup: Miscellaneous

The LHCb trigger and dataset

Running conditions in most of 2012

- LHC: 20 MHz bunch crossing
- Luminosity: $4.0 \times 10^{32} \text{ cm}^{-2} \text{s}^{-1}$, using luminosity leveling
- Visible interactions rate: 12.0 - 14.0 MHz
- L0 output rate: 950 kHz
- HLT output rate: 4.5 kHz
- Event size: 60 kB



37 pb^{-1} acquired in 2010

1 fb^{-1} acquired in 2011

2 fb^{-1} acquired in 2012

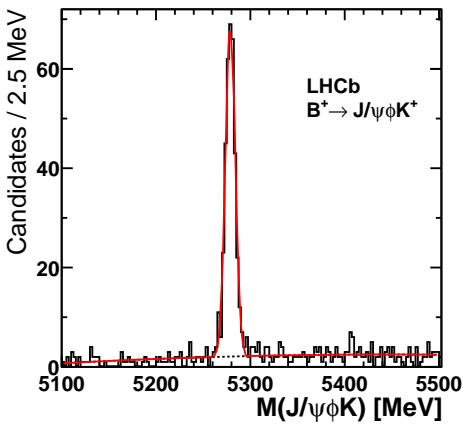
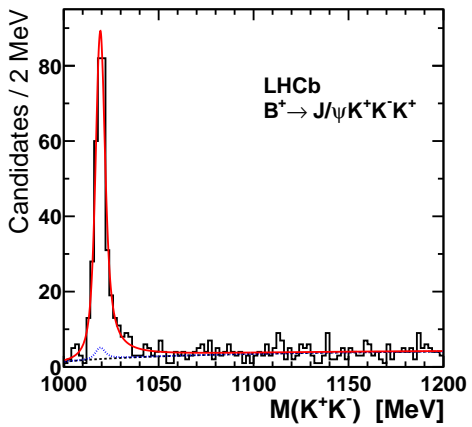
X(3872) mass measurement at LHCb: uncertainties

Source of uncertainty	$\Delta\sigma/\sigma [\%]$
$X(3872)$ polarization	2.1
$X(3872)$ decay model	1.0
$X(3872)$ decay width	5.0
Mass resolution	5.8
Background model	6.4
Tracking efficiency	7.4
Track χ^2 cut	2.0
Vertex χ^2 cut	3.0
Muon trigger efficiency	2.9
Global event cuts	3.0
Muon identification	1.1
Integrated luminosity	3.5
$J/\psi \rightarrow \mu^+\mu^-$ branching fraction	1.0
Total	14.3

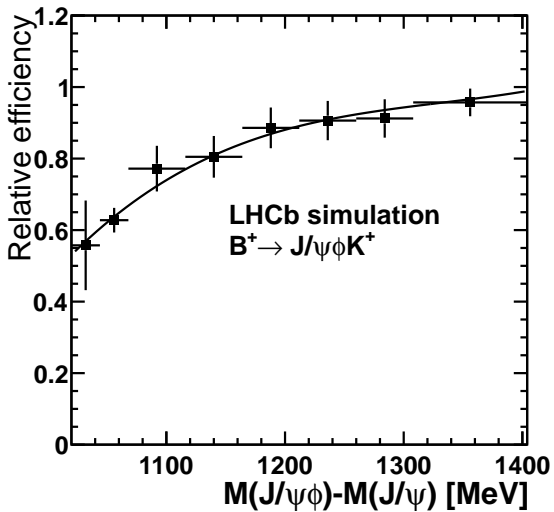
Category	Source of uncertainty	Δm [MeV/ c^2]
	$\psi(2S)$	$X(3872)$
Mass fitting	Natural width	–
	Radiative tail	0.02
	Resolution	–
	Background model	0.02
Momentum calibration	Average momentum scale	0.08
	η dependence of momentum scale	0.02
Detector description	Energy loss correction	0.05
Detector alignment	Track slopes	0.01
Total		0.10
		0.12

Search for X(4140) and X(4274) at LHCb

- LHCb searched for X(4140) and X(4274) in a sample with 0.376 fb^{-1} of 2011 dataset [Ref. Phys. Rev. D 85, 091103(R) (2012)].
- Background subtracted sample with 382 ± 22 $B^\pm \rightarrow J/\psi \phi K^\pm$ events



Search for X(4140) and X(4274) at LHCb: efficiency



X(3872) quantum numbers: previous measurements

CDF

- Sample dominated by prompt X(3872)
- 3D analysis: fit to $\pi^+\pi^-$ and J/ψ helicity angles and the angle between the $\pi^+\pi^-$ and J/ψ decay planes
- $X(3872)$ J^{PC} constrained to 1^{++} or 2^{-+}
- Phys.Rev.Lett.98:132002 (2007)

BaBar

- Observed 34 ± 7 $X(3872) \rightarrow \omega J/\psi$
- Study of $\omega \rightarrow \pi^-\pi^+\pi^0$ mass distribution favoured 2^{-+} , but 1^{++} was not ruled out.
- arXiv:1005.5190, Phys. Rev. D 82, 011101(R) (2010)

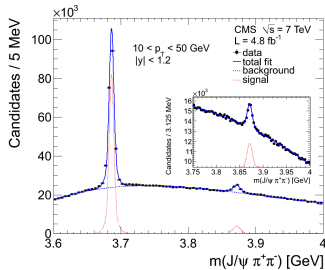
Belle

- Observed 173 ± 16 $B \rightarrow X(3872)K$, with $X(3872) \rightarrow J/\psi\pi^+\pi^-$ and $J/\psi \rightarrow \mu^+\mu^-$
- By studying one-dimensional distributions in three different angles, Belle concluded that their data were equally well described by the 1^{++} and 2^{-+} hypotheses.
- arXiv:1107.0163, Phys. Rev. D 84, 052004 (2011)

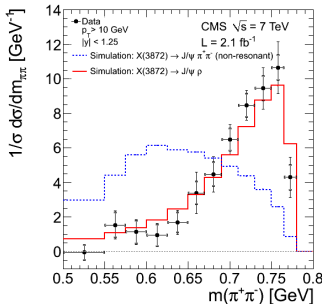
X(3872) production studies at CMS

CMS collaboration performed detailed X(3872) production studies using the decay mode $X(3872) \rightarrow J/\psi \pi^+ \pi^-$, with $J/\psi \rightarrow \mu^+ \mu^-$ and 4.1 fb^{-1} $\sqrt{s} = 7 \text{ TeV}$

- Measurements are performed in the range $10 < p_T^{X(3872)} < 50 \text{ GeV}$ and rapidity $|y| < 1.2$.
- Detailed study of the dipion mass showing the decay proceeds dominantly through a intermediate ρ

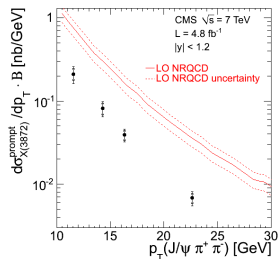
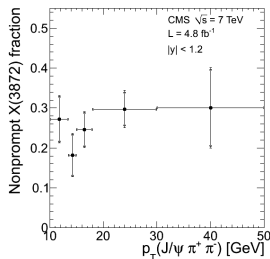
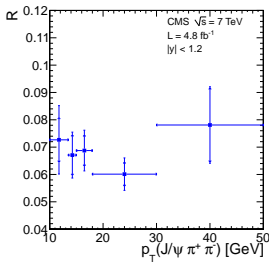


[arXiv:1302.3968]



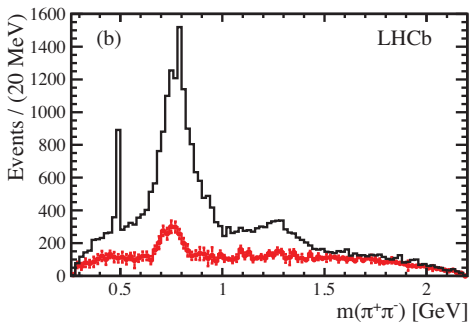
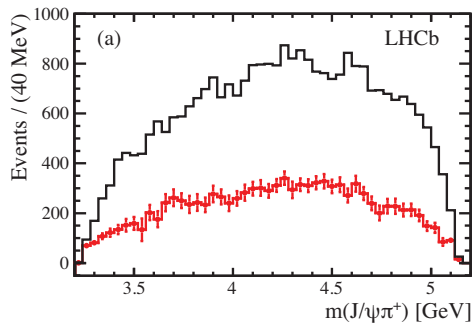
X(3872) production studies at CMS

- Ratio of the X(3872) and $\psi(2S)$ cross sections times their branching fractions into $J/\psi\pi^+\pi^-$ measured in function of p_T .
- Fraction of X(3872) originating from B decays.
- Prompt X(3872) differential cross section times branching fraction into $J/\psi\pi^+\pi^-$ and comparison with theory prediction.



[arXiv:1302.3968]

$J/\psi \pi^+$ mass in $B^0 \rightarrow J/\psi \pi^+ \pi^-$



Spectroscopy in light quark sector: $B^0 \rightarrow J/\psi \pi^+ \pi^-$

Phys. Rev. D 87, 052001

- The substructure of mesons belonging to the scalar nonet is controversial.
- Many possibilities: $q\bar{q}$, $q\bar{q}q\bar{q}$, mixtures etc.
- $q\bar{q}$ case:

$$|f_0(980)\rangle = \cos \varphi_m |s\bar{s}\rangle + \sin \varphi_m |n\bar{n}\rangle$$

$$|f_0(500)\rangle = -\sin \varphi_m |s\bar{s}\rangle + \cos \varphi_m |n\bar{n}\rangle,$$

$$\text{where } |n\bar{n}\rangle \equiv \frac{1}{\sqrt{2}} (|u\bar{u}\rangle + |d\bar{d}\rangle).$$

- $q\bar{q}q\bar{q}$ case:

$$|f_0(980)\rangle = \frac{1}{\sqrt{2}} (|[su][\bar{s}\bar{u}]\rangle + |[sd][\bar{s}\bar{d}]\rangle)$$

$$|f_0(500)\rangle = |[ud][\bar{u}\bar{d}]\rangle.$$

- Observable of interest for both cases:

$$\tan^2 \varphi_m \equiv r_\sigma^f = \frac{\mathcal{B}(\bar{B}^0 \rightarrow J/\psi f_0(980))}{\mathcal{B}(\bar{B}^0 \rightarrow J/\psi f_0(500))} \frac{\Phi(500)}{\Phi(980)}$$

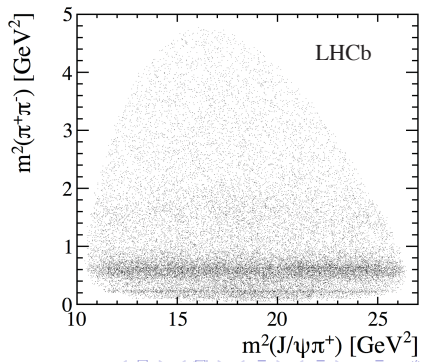
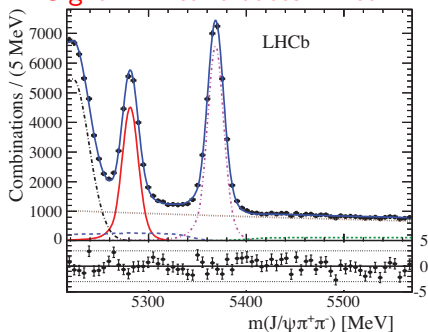
- Prediction for tetraquark states: $r_\sigma^f = 1/2$ [PRL 111, 062001 (2013)]

Amplitude analysis of $B^0 \rightarrow J/\psi \pi^+ \pi^-$

Phys. Rev. D 87, 052001

- Approach similar to the $Z(4430)^+$ analysis: 4D matrix element describing $\pi^+ \pi^-$ resonances;
- No evidence of $J/\psi \pi^+$ resonances
- 19,000 B^0 signal candidates
- Background modelled from sidebands

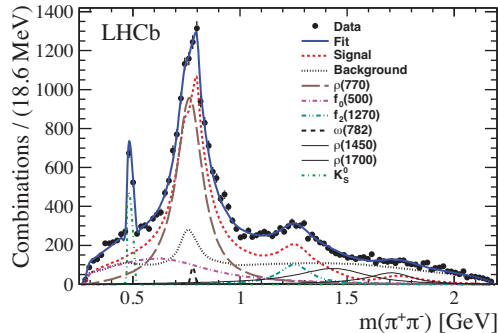
Signal B^0 candidates in red.



Amplitude analysis of $B^0 \rightarrow J/\psi \pi^+ \pi^-$

Phys. Rev. D 87, 052001

R	$\mathcal{B}(\bar{B}^0 \rightarrow J/\psi R, R \rightarrow \pi^+ \pi^-)$
$\rho(770)$	$(2.50 \pm 0.10^{+0.18}_{-0.15}) \times 10^{-5}$
$f_0(500)$	$(8.8 \pm 0.5^{+1.1}_{-1.5}) \times 10^{-6}$
$f_2(1270)$	$(3.0 \pm 0.3^{+0.2}_{-0.3}) \times 10^{-6}$
$\omega(782)$	$(2.7^{+0.8+0.7}_{-0.6-0.5}) \times 10^{-7}$
$\rho(1450)$	$(4.6 \pm 1.1 \pm 1.9) \times 10^{-6}$
$\rho(1700)$	$(2.0 \pm 0.5 \pm 1.2) \times 10^{-6}$



- Best fit model shows does not require $f_0(980)$ component.
- Upper limit on the $f_0(500) - f_0(980)$ mixing angle.
- Different from tetraquark prediction (1/2) by 8σ

$$\tan^2 \varphi_m \equiv r_\sigma^f = (1.1^{+1.2+6.0}_{-0.7-0.7}) \times 10^{-2} < 0.098 \text{ at } 90\% \text{ C.L}$$